JOC Article

Origin of Chemiluminescence Accompanying the Reaction of the 9-Cyano-10-methylacridinium Cation with Hydrogen Peroxide

A. Wróblewska,[†] O. M. Huta,[‡] S. V. Midyanyj,[‡] I. O. Patsay,[‡] J. Rak,[†] and J. Błażejowski*,[†]

Faculty of Chemistry, University of Gdańsk, J. Sobieskiego 18, 80-952 Gdańsk, Poland, and Faculty of Chemistry, Ivan Franko L'viv National University, Kyrylo and Mefodiy 6, 79005 L'viv, Ukraine

bla@chem.univ.gda.pl

Received October 1, 2003

The 9-cyano-10-methylacridinium cation possesses an electrophilic center at the carbon atom in position (9) susceptible to the addition of anions. The addition of OOH^- to this cation—in weakly acidic, neutral, or alkaline media—initiates processes leading to the formation of electronically excited 10-methyl-9-acridinone, which deactivates by light emission. The effect of changes in reactant concentrations and pH on emission decay with time, as well as other features of the accompanying chemiluminescence, were established. Calculations carried out at the semiempirical and density functional theory level demonstrated that initial addition of OOH^- and subsequent processes lead either to the elimination of OCNH (in weakly acidic and neutral media) or OCN^- (in alkaline media) and that their exothermicity is sufficiently high to generate electronically excited 10-methyl-9-acridinone. On the other hand, primary addition of OH^- to C(9) in alkaline media initiates the conversion of the cation to the nonexcited 10-methyl-9-acridinone. This relatively rapid process influences to a substantial extent the intensity of the chemiluminescence. The prospects for the analytical application of 9-cyano-10-methylacridinium salts are briefly outlined.

1. Introduction

Among the numerous chemical processes that lead to chemiluminescence, of importance are those occurring with the involvement of 10-methylacridinium derivatives, usually substituted at the carbon atom (9).[1−10] These compounds are relatively easily oxidized with hydrogen peroxide,[3,4,6,8,9,11] other peroxides,[12] persulfates,[13] or molecular oxygen[14−19] in neutral or alkaline media. The oxidation leads to a larger or smaller number of electronically excited 10-methyl-9-acridinone (MA*) molecules that emit light upon radiative deactivation.[1−19] The emission is influenced by numerous organic and inorganic substances, and this constitutes a basis for the analytical application of 10-methylacridinium derivatives.[7,9,10,20] On the other hand, 10-methylacridinium chemiluminogens are widely used as fragments of chemiluminescent labels which have been successfully applied in medical, biochemical, and environmental analyses.[4,6,9,10] These are the reasons for our interest in 9-cyano-10-methylacridinium cation (CMA^+), which has not been very thoroughly investigated from this point of view.

The 9-cyano-10-methylacridinium cation (Chart 1) has long been known as a component of acridinium salts.[21−23] Quite recently, we determined the structure of 9-cyano-10-methylacridinium hydrogen dinitrate in the crystalline phase,[24] which encouraged us to undertake investigations into the chemiluminescent properties of CMA^+.

* Corresponding author. Phone: +48 58 345 03 31. Phone/fax: +48 58 345 04 64.
[†] University of Gdańsk.
[‡] Ivan Franko L'viv National University.

(1) Rauhut, M. M. *Acc. Chem. Res.* **1969**, *2*, 80.
(2) White, E. H.; Roswell, D. F. *Acc. Chem. Res.* **1970**, *3*, 541.
(3) McCapra, F. *Acc. Chem. Res.*, **1976**, *9*, 201.
(4) Weeks, I.; Beheshti, I.; McCapra, F.; Campbell, A. K.; Woodhead, J. S. *Clin. Chem.* **1983**, *29*, 1474.
(5) Abdel-Lalif, M. S.; Guilbault, G. G. *Anal. Chem.* **1988**, *60*, 2671.
(6) Zomer G.; Stavenuiter, J. F. C.; Van den Berg, R. H.; Jansen, E. H. J. M. *Pract. Spectrosc.* **1991**, *12*, 505.
(7) Warner, I. M.; Soper, S. A.; McGown, L. B. *Anal. Chem.* **1996**, *68*, 73R.
(8) Rak, J.; Skurski, P.; Blazejowski, J. *J. Org. Chem.* **1999**, *64*, 3002.
(9) Dodeigne, C.; Thunus, L.; Lejeune, R. *Talanta* **2000**, *51*, 415.
(10) Zomer, G.; Jacquemijns, M. In *Chemiluminescence in Analytical Chemistry*; Garcia-Campana, A. M., Baeyens, W. R. G., Eds.; Marcel Dekker: New York, 2001; p 529.
(11) White, E. H.; Roswell, D. F.; Dupont, A. C.; Wilson, A. A. *J. Am. Chem. Soc.* **1987**, *109*, 5189.
(12) Sakanishi, K.; Kato, Y.; Mizukoshi, E.; Shimizu, K. *Tetrahedron Lett.* **1994**, *35*, 4789.
(13) Cass, M. W.; Rapaport, E.; White, E. H. *J. Am. Chem. Soc.* **1972**, *94*, 3168.
(14) Happ, J. W.; Janzen, E. G.; Rudy, B. C. *J. Org. Chem.* **1970**, *35*, 3382.
(15) Happ, J. W.; Janzen, E. G. *J. Org. Chem.* **1970**, *35*, 3396.
(16) Rapaport, E.; Cass, M. W.; White, E. H. *J. Am. Chem. Soc.* **1972**, *94*, 3160.
(17) Suzuki, N.; Kazui, Y.; Kato, M.; Izawa, Y. *Heterocycles* **1981**, *16*, 2121.
(18) Suzuki, N.; Kazui, Y.; Tsukamoto, T.; Kato, M.; Izawa, Y. *Bull. Chem. Soc. Jpn.* **1983**, *56*, 1519.
(19) Kamiya, I.; Sugimoto, T.; Yamabe, K. *Bull. Chem. Soc. Jpn.* **1984**, *57*, 1735.
(20) Rokicioglu, Y.; Schulman, J. M.; Schulman, S. G. In *Chemiluminescence in Analytical Chemistry*: Garcia-Campana, A. M., Baeyens, W. R. G., Eds.; Marcel Dekker: New York, 2001; p 105.
(21) Kaufmann, C.; Albertini, A. *Ber. Dtsch. Chem. Ges.* **1909**, *42*, 1999, 2002.
(22) Kaufmann, C.; Albertini, A. *Ber. Dtsch. Chem. Ges.* **1911**, *44*, 2052.
(23) McCapra, F.; Richardson, D. G. *Tetrahedron Lett.* **1964**, 3167.
(24) Huta, O. M.; Patsaj, I. P.; Konitz, A.; Meszko, J.; Blazejowski, J. *Acta Crystallogr., Sect. C* **2002**, *C58*, o295.

10.1021/jo0354387 CCC: $27.50
Published on Web 02/11/2004

CHART 1. Canonic Structure of CMA^+ with the Numbering of Atoms Indicated

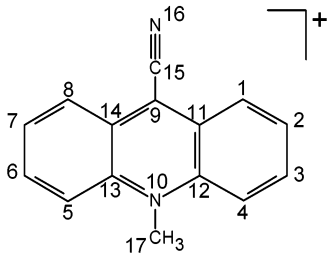

We had come across an early publication by Radziszewski, who reported for the first time that chemiluminescence accompanies the reaction of the synthetic organic compound lophine (2,4,5-triphenyl-1*H*-imidazole) with oxygen in strongly alkaline media.[25] Later on, McCapra et al.[23,26] found that oxidation of CMA^+ with hydrogen peroxide in alkaline water−ethanolic media produces light. Others noted that the chemiluminescence accompanying the oxidation of 10-methylacridinium cations with O_2 in aqueous alkaline media is enhanced in the presence of KCN.[14,15,17] The emitting entity was always MA*. This brief overview indicates that little is known about the origin of the chemiluminescence produced by CMA^+. We thus undertook investigations in order to discover the behavior of CMA^+ and the principal features of the chemiluminescence accompanying its reaction with hydrogen peroxide. We further carried out calculations in order to discover the principal reaction pathways. Last, we explored the possible analytical uses of CMA^+.

2. Methods

2.1. Synthesis. 9-Cyano-10-methylacridinium hydrogen dinitrate was prepared by the oxidation of 9-cyano-10-methylacridan[21,22] with dilute nitric acid.[23] The compound was identified by the X-ray method.[24]

2.2. Chemiluminescence and Spectral Investigations. Chemiluminescence investigations were carried out using a "homemade" spectrochemiluminometer—a spectrofluorometer modified by using high brightness optics, a collimating sphere, and a sensitive photomultiplier (for the 320−650 nm region). All measurements were done in a quartz cuvette of 1 cm optical length and 10 mL volume. Initially, known volumes of 10^{-4}−10^{-6} M CMA^+ in 10^{-3} M HNO_3 were mixed with known volumes of 4−10^{-6} M H_2O_2 in water. Next, 4 mL of this mixture was poured into the cuvette, which was then placed in the spectrochemiluminometer compartment. After this, 1 mL of buffer or an appropriate aqueous solution of NaOH was added to the cuvette, which initiated chemiluminescence. This moment was taken as the initial time in all experiments. The following buffers were used: CH_3COOH/CH_3COONa (pH = 4−5), NaH_2PO_4/Na_2HPO_4 (pH = 5−8), H_3BO_3/NaOH (pH = 8−10), $NaHCO_3/Na_2CO_3$ (pH = 10−11) and the appropriate NaOH solutions (pH > 11). Only during the recording of chemiluminescence spectra did the emitted radiation pass through a monochromator. In other experiments, the whole radiation was directed to the photomultiplier.

Absorption spectra were recorded in 1 cm quartz cuvettes.

2.3. Calculations. Unconstrained geometry optimizations employing the EF algorithm[27] were performed at the level of the semiempirical PM3[28] and PM3/CI,[29] as well as the density functional theory (DFT)[30] level with the 6-31G** basis set.[31] The density functional calculations were carried out with the hybrid B3LYP functional.[32−34] After completion of each optimization, the Hessian matrix was calculated[30,31] to check the nature of the stationary point and to compute the vibrational frequencies. PM3 was chosen since it performs better than other MNDO-type semiempirical methods.[35] It also supplied the initial structures for the DFT geometry optimizations. The use of two independent methods (PM3 and DFT) provided a broader insight into the mechanism of the ongoing processes. The solvent effect was included in the PM3 calculations by means of the conductor-like screening model (COSMO) (assuming molecular shape cavity).[36] In the DFT approach, the presence of solvent was modeled at the level of the polarized continuum model (PCM) (UAHF radii were used to obtain the molecular cavity),[37,38] in which single-point calculations were carried out for the structures optimized in the gaseous phase. The zero-point energy, thermal contributions to energy from vibrations, rotations, and translations, and also the entropy term were calculated in the rigid-rotor harmonic-oscillator approximation[39] using standard statistical thermodynamics routines.[40] These terms were subsequently used to convert the electronic energy into enthalpy and Gibbs' free energy at an ambient temperature of 298.15 K and a pressure of 1 atm. The PM3 (PM3(COSMO)) and the PM3/CI calculations were carried out using the MOPAC 2000 molecular orbital package[41] and the DFT (DFT(PCM))-GAUSSIAN 98 program package.[42] DFT calculations were partially

(25) Radziszewski, B. *Ber. Dtsch. Chem. Ges.* **1877**, *10*, 70.
(26) McCapra, F.; Richardson, D. G.; Chang, Y. C. *Photochem. Photobiol.* **1965**, *4*, 1111.
(27) Baker, J. *J. Comput. Chem.* **1986**, *7*, 385.
(28) Stewart, J. J. P. *J. Comput. Chem.* **1989**, *10*, 209, 221.
(29) Armstrong, D. R.; Fortune, R.; Perkins, P. G.; Stewart, J. J. P. *J. Chem. Soc., Faraday Trans. 2* **1972**, *68*, 1839.
(30) *Density Functional Methods in Chemistry*; Labanowski, K. J., Andzelm, J. W., Eds.; Springer-Verlag: New York, 1991.
(31) Hehre, W. J.; Radom, L.; Schleyer, P. v. R.; Pople, J. A. *Ab initio Molecular Orbital Theory*; Wiley: New York, 1986.
(32) Becke, A. D. *Phys. Rev. A* **1988**, *38*, 3098.
(33) Becke, A. D. *J. Chem. Phys.* **1993**, *98*, 1372, 5648.
(34) Lee, C.; Yang, W.; Parr, R. G. *Phys. Rev. B* **1988**, *37*, 785.
(35) Stewart, J. J. P. *J. Comput.-Aided Mol. Des.* **1990**, *4*, 1.
(36) Klamt, A.; Schuurmann, G. Z. *J. Chem. Soc., Perkin Trans. 2* **1993**, 799.
(37) Tomasi, J.; Persico, M. *Chem. Rev.* **1994**, *94*, 2027.
(38) Barone, V.; Cossi, M.; Mennucci, B.; Tomasi, J. *J. Chem. Phys.* **1997**, *107*, 3210.
(39) Baer, T.; Hase, W. L. *Unimolecular Reaction Dynamics*; Oxford University Press: New York, 1996.
(40) Dewar, M. J. S.; Ford, G. P. *J. Am. Chem. Soc.* **1977**, *99*, 7822.
(41) Stewart, J. J. P. *MOPAC 2000*; Fujitsu Ltd.: Tokyo, Japan, 1999.
(42) Frish, M. J.; Trucks, G. W.; Schlegel, H. B.; Scuseria, G. E.; Robb, M. A.; Cheeseman, J. R.; Zakrzewski, V. G.; Montgomery, J. A.; Stratmann, R. E.; Burant, J. C.; Dapprich, S.; Millam, J. M.; Daniels, A. D.; Kudin, K. N.; Strain, M. C.; Farkas, O.; Tomasi, J.; Barone, V.; Cossi, M.; Cammi, R.; Mennucci, B.; Pomelli, C.; Adamo, C.; Clifford, S.; Ochterski, J.; Petersson, G. A.; Ayala, P. Y.; Cui, Q.; Morokuma, K.; Malick, D. K.; Rabuck, A. D.; Raghavachari, K.; Foresman, J. B.; Cioslowski, J.; Ortiz, J. V.; Baboul, A. G.; Stefanov, B. B.; Liu, G.; Liashenko, A.; Piskorz, P.; Komaromi, I.; Gomperts, R.; Martin, R. L.; Fox, D. J.; Keith, T.; Al-Laham, M. A.; Peng, C. Y.; Nanayakkara, A.; Challacombe, M.; Gill, P. M. W.; Johnson, B.; Chen, W.; Wong, M. W.; Andres, J. L.; Gonzalez, C.; Head-Gordon, M.; Replogle, E. S.; Pople, J. A. *GAUSSIAN 98*, Revision A.9; Gaussian, Inc.: Pittsburgh, PA, 1998.

SCHEME 1. Pathways of the Reactions of CMA^+ with OOH^- [a]

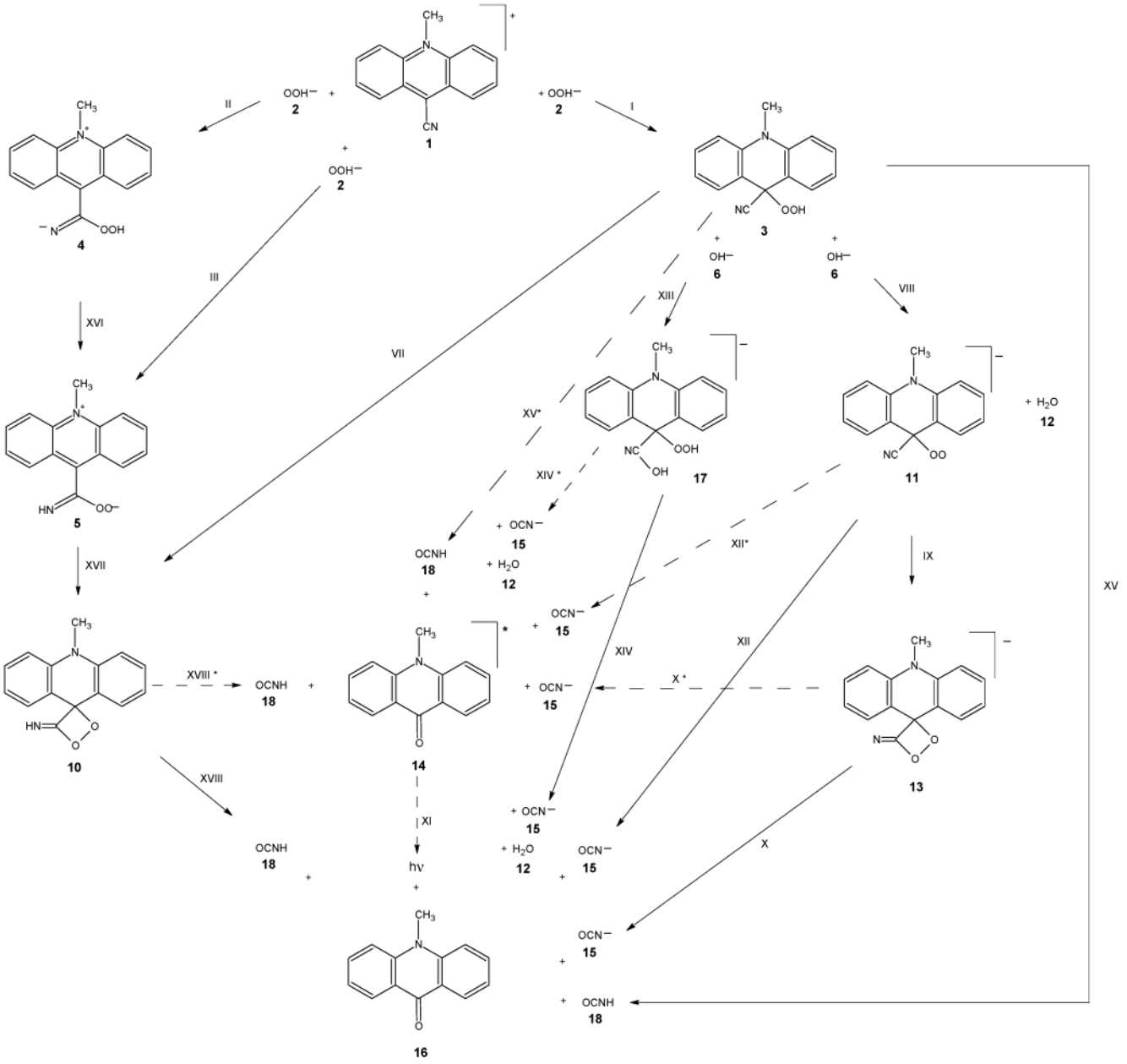

[a] The solid arrows indicate processes involving molecules in the ground electronic state for which both thermodynamic and kinetic characteristics were theoretically predicted, while the dashed arrows indicate hypothetical steps involving electronically excited 10-methyl-9-acridinone molecules for which only thermodynamic data could be obtained.

done on the computers of the Tri-City Academic Computer Network Center in Gdańsk, Poland (TASK).

The theoretically obtained characteristics enable determination of the enthalpies ($\Delta_{r,298}H°$) and Gibbs' free energies (free energies in the case of DFT(PCM)) ($\Delta_{r,298}G°$) of the reactions (r), as well as the enthalpies ($\Delta_{a,298}H°$) and Gibbs' free energies (free energies in the case of DFT(PCM)) ($\Delta_{a,298}G°$) of the activation (a) indicated in Scheme 1, by following the basic rules of thermodynamics.[43] Complete thermodynamic and kinetic (activation barriers) characteristics were predicted only for steps involving molecules in the ground electronic state (indicated by solid-line arrows in Schemes 1 and 2). However, to obtain some idea of how electronically excited 10-methyl-9-acridinone could be formed, we calculated (only thermodynamic) data for the steps involving MA* (indicated in Scheme 1 by dashed arrows). The rate constants ($_{298}k°$) for the gaseous phase reactions were obtained by applying the equation

$$_{298}k° = \frac{RT}{Nh}\exp[-\Delta_{a,298}G°/(RT)]$$

resulting from transition state theory, and the reaction completion time ($_{298}\tau_{99}$) from the formula

$$_{298}\tau_{99} = \ln 100/{}_{298}k°$$

(43) Atkins, P. W. *Physical Chemistry*, 5th ed.; Oxford University Press: Oxford, U.K., 1994.

SCHEME 2. Pathways of the Reactions of CMA^+ with OH^-

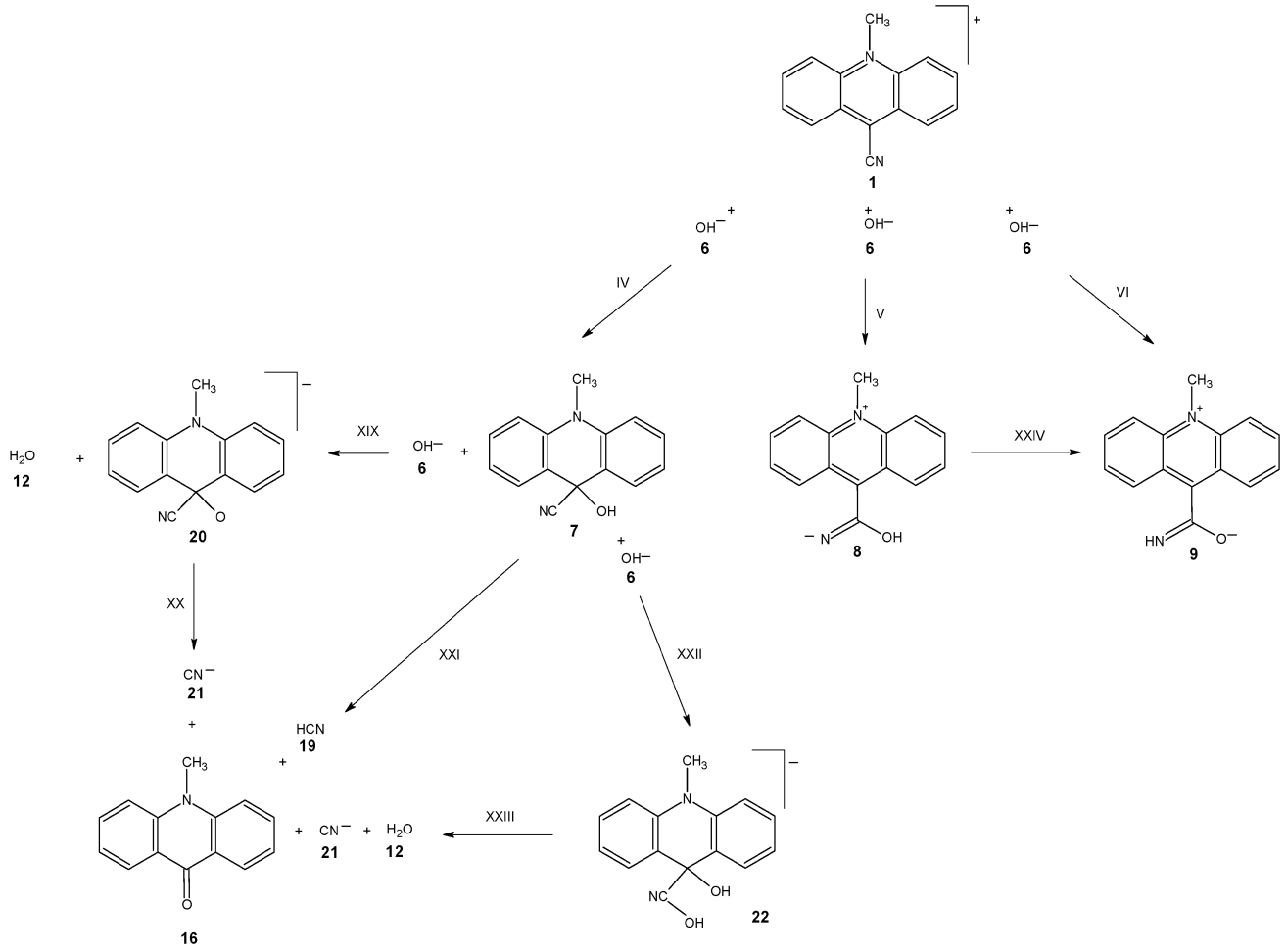

where R, T, N, and h denote the gas constant, temperature (298.15 K), Avogadro number, and Planck's constant, respectively.[8,43]

3. Results and Discussion

3.1. Chemiluminescence Accompanying the Reaction of CMA^+ with Hydrogen Peroxide. The interaction of CMA^+ with H_2O_2 in weakly acidic, neutral, or alkaline media produces MA*, whose radiative deactivation is responsible for the chemiluminescence phenomena (Figure 1).[44,45] The emission increases with time (Figures 1 and 2), reaches a maximum, and decays within hours in weakly acidic media or within minutes in weakly alkaline media (Figure 2). In moderately alkaline media, chemiluminescence is completed in under 1 min. The total integral intensity of emission (I_{total}) changes with pH (Figure 3) and H_2O_2 concentration (Figure 4). In all cases, very similar maximum values of I_{total} are reached at various abscissal values. The latter two dependencies form a basis for the selection of the most suitable conditions for analytical measurements.

CMA^+ exhibits relatively strong absorption with maxima at 265 and 385 nm (Figure 5). These bands diminish in the presence of alkaline H_2O_2; at the same time, however, a new band appears with a maximum at 330 nm. This band can be attributed to the product of the primary addition of OOH^- to CMA^+.

3.2. Behavior of CMA^+ in Alkaline Media. CMA^+ is quite efficiently converted to MA in moderately alkaline media without light emission (Figure 6). With its rate constant of 560 M^{-1} s^{-1}, this unwanted bimolecular reaction is thus relatively fast.[45] It is believed to be the major cause of the reduced quantum yields of chemiluminescence accompanying the oxidation of 10-methylacridinium cations.[1−3,6,8,9,45]

3.3. Origin of Chemiluminescence Due to the Reaction of CMA^+ with Hydrogen Peroxide. The primary steps of the reactions of CMA^+ with either OOH^- or OH^- are determined mainly by the location of the electrophilic center in the cation. As indicated by the frontier orbital theory,[46] LUMO distribution of an electrophilic species determines molecular centers sensitive to nucleophilic attack. The value of the LCAO coefficient of the p_z atomic orbital in CMA^+'s LUMO is ca. 10 times higher at the endocyclic C(9) than at the cyano group carbon atom (0.31 and 0.03, respectively). This implies that C(9) rather than the carbon atom of the cyano group is the site of the primary nucleophilic attack of the above-

(44) Bouzyk, A.; Jozwiak, L.; Kolendo, A. Yu.; Blazejowski, J. *Spectrochim. Acta, Part A* **2003**, *59*, 543.
(45) Wroblewska, A.; Huta, O. M.; Patsay, I. O.; Petryshyn, R. S.; Blazejowski, J. *Anal. Chim. Acta*, in press (paper ACA225049).
(46) Fleming, I. *Frontier Orbitals and Organic Chemical Reactions*; Wiley: London, New York, 1976.

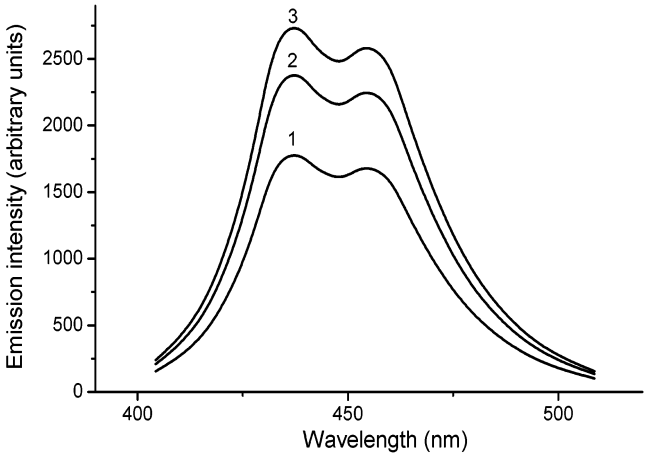

FIGURE 1. Spectra of the chemiluminescence accompanying the reaction of CMA^+ (2.5×10^{-5} M) with H_2O_2 (2.0 M) at pH = 6.1 recorded at 110−135 (**1**), 160−185 (**2**), and 215−240 (**3**) time intervals (in s) following the mixing of the reagents.

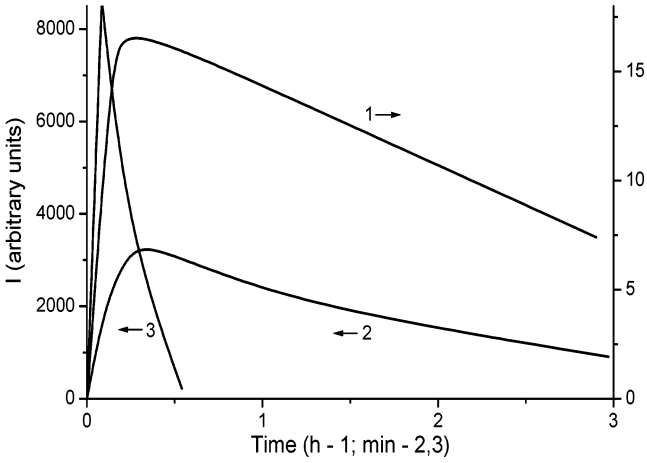

FIGURE 2. Integral intensity (corresponding to the whole spectrum) of the chemiluminescence (I) accompanying the reaction of CMA^+ (5.0×10^{-7} M) with H_2O_2 (0.1 M) at pH: 5.5 (**1**), 9.5 (**2**), and 11.1 (**3**) versus time following the mixing of the reagents.

mentioned anions, despite the fact that the Mulliken partial charge (DFT level) at C(9) is lower than at C(16) (0.17 and 0.25, respectively).

Another premise which must be taken into account is the fact that H_2O_2 reacts spontaneously with OH^- to yield OOH^- (the thermodynamic data (in kcal/mol) for the reaction $H_2O_2 + OH^- \rightarrow H_2O + OOH^-$ are: −26.8 ($\Delta_{r,298}H°$; DFT), −27.8 ($\Delta_{r,298}G°$; DFT) and −1.7 ($\Delta_{r,298}G°$; DFT(PCM)).

Taking into account the reaction pathways proposed by other authors,[14,15,17,23,26] as well as the information mentioned above, we considered the processes which explain the experimental findings and are in accordance with general chemical knowledge. The pathways of the possible reactions of CMA^+ with OOH^- and OH^-, outlined in Schemes 1 and 2, respectively, emerge from a thorough analysis of the results of theoretical calculations. Pathway one represents the attack of OOH^- on carbon atom (9) of CMA^+ (**1**) (step I), followed by the reaction of the addition product (**3**) with OH^- (step VIII), the cyclization of the anion so formed (**11**) to dioxoethane (**13**) (step IX),

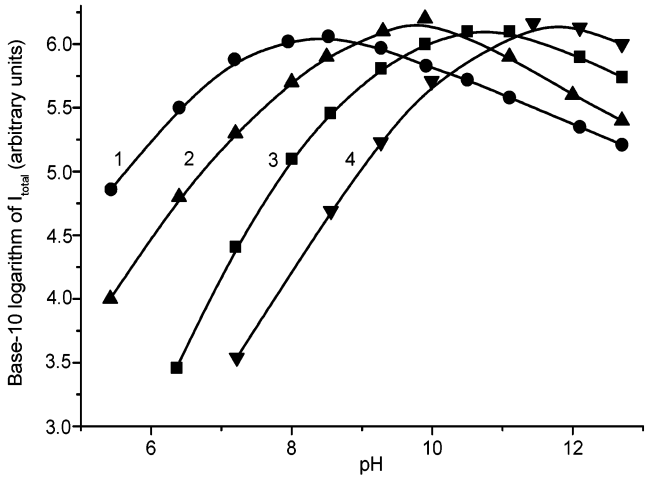

FIGURE 3. Total integral intensity (corresponding to the whole spectrum and emission time) of the chemiluminescence (I_{total}) accompanying the reaction of CMA^+ (5.0×10^{-7} M) with H_2O_2 (concentration in M: 1.0 (**1**); 0.1 (**2**); 0.01 (**3**); 0.0001 (**4**)) as a function of pH.

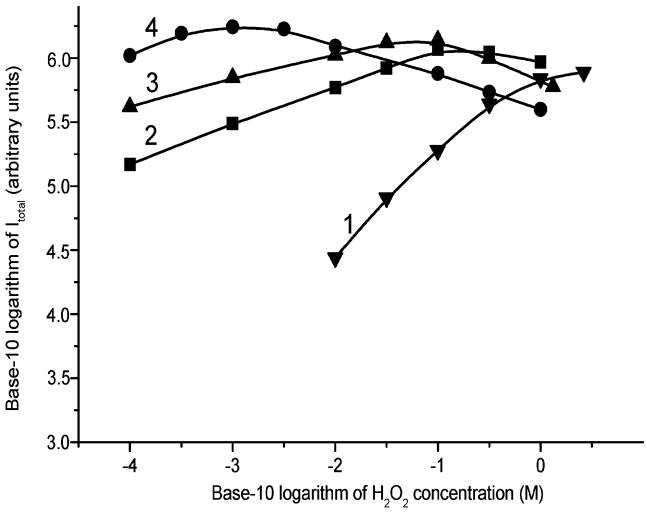

FIGURE 4. Total integral intensity (corresponding to the whole spectrum and emission time) of the chemiluminescence (I_{total}) accompanying the reaction of CMA^+ (5.0×10^{-7} M) with H_2O_2, at various concentrations, at pH: 7.2 (**1**); 9.2 (**2**); 9.9 (**3**); and 11.0 (**4**).

and the elimination of OCN^- leading to MA* (**14**) (step X*). Pathway two assumes the attack of OH^- on the carbon atom of the cyano group in **3** (step XIII) and the subsequent simultaneous elimination of OCN^- and H_2O from the intermediate thus formed (**17**), leading to MA* (step XIV*). The possible addition of OH^- to the carbon atom of the cyano group of **3** has been postulated by other authors.[47] The process is probable since the LCAO coefficients of s and p_z atomic orbitals of C(15) in LUMO afford the substantial values of 0.19 and 0.08, respectively. Moreover, the Mulliken partial charge (DFT level) at C(15) in **3** is equal to 0.36, which further indicates such a possibility. Pathway three assumes that the addition product (**3**) undergoes cyclization to **10** (step VII), this reaction being followed by the elimination of OCNH to

(47) Acheson, R. M. *Acridines*, 2nd ed.; J. Wiley and Sons: New York, 1973.

TABLE 1. Thermodynamic Data (in kcal/mol) for the Elementary Steps of the Reactions of CMA^+ with OOH^- and OH^- [a]

step no.	gaseous phase				aqueous phase	
	$\Delta_{r,298}H°$		$\Delta_{r,298}G°$		$\Delta_{r,298}H°$	$\Delta_{r,298}G°$
(Schemes 1 and 2)	PM3	DFT	PM3	DFT	PM3 (COSMO)	DFT (PCM)
I	−163.7	−165.5	−152.0	−153.2	−5.1	−43.9
II	−114.5		−102.1		1.7	
III	−106.0	−142.5	−92.9	−129.2	1.8	−30.5
IV	−192.2	−188.7	−182.5	−178.2	−24.1	−49.9
V	−141.6		−131.3		−12.8	
VI	−155.4	−181.6	−145.5	−171.6	−27.7	−47.6
VII	8.8	−2.8	10.5	−1.3	11.0	−1.0
VIII	−45.4	−65.9	−44.9	−66.4	−8.8	−16.4
IX	4.8		4.8		5.9	
X	−94.2		−106.6		−103.1	
X*	−11.9		−24.9		−28.5	
XI	−82.3		−81.8		−74.6	
XII	−89.4	−95.9	−101.8	−107.1	−97.2	−107.5
XII*	−7.1		−20.1		−22.6	
XIII	−41.0	−53.9	−31.4	−42.8	−14.0	−1.3
XIV	−78.5	−107.9	−101.8	−130.7	−97.5	−122.6
XIV*	−11.4		−33.6		−17.4	
XV	−69.5	−90.0	−81.7	−101.6	−79.1	−91.4
XV*	12.8		0.1		−4.5	
XVI	8.5		9.2		0.1	
XVII	−48.9	−25.8	−48.7	−25.3	4.2	−14.3
XVIII	−78.3	−87.3	−92.2	−100.3	−90.1	−90.4
XVIII*	4.0		−10.4		−15.5	
XIX	−55.3	−73.8	−56.4	−74.9	−11.0	−26.3
XX	14.9	6.5	3.7	−4.6	−3.2	−10.4
XXI	0.7	−10.0	−10.6	−21.0	−6.0	−5.5
XXII	−53.5	−77.9	−42.9	−66.6	−9.6	−19.5
XXIII	13.0	10.6	−9.8	−12.9	−4.6	−17.2
XXIV	−13.8		−14.2		−14.9	

[a] $\Delta_{r,298}H°$ and $\Delta_{r,298}G°$, respectively, represent the enthalpy and Gibbs' free energy (gaseous phase) or free energy (aqueous phase) of the reaction corresponding to the relevant step number at temperature 298.15 K and standard pressure (1 atm). [b] The thermodynamic characteristics correspond to the processes proceeding in the ground electronic state and the hypothetical steps (indicated by an asterisk) involving 10-methyl-9-acridinone molecules in the electronically excited state.

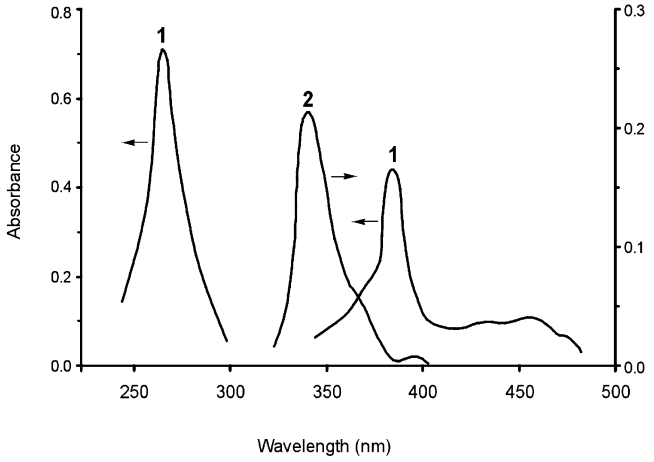

FIGURE 5. Absorption spectra of CMA^+ (1.0×10^{-5} M) at pH = 3 (**1**) and the probable product of the addition of OOH^- to it (**2**) ($CMA^+ = 2.5 \times 10^{-5}$ M; $H_2O_2 = 1.5$ M; pH = 8.1).

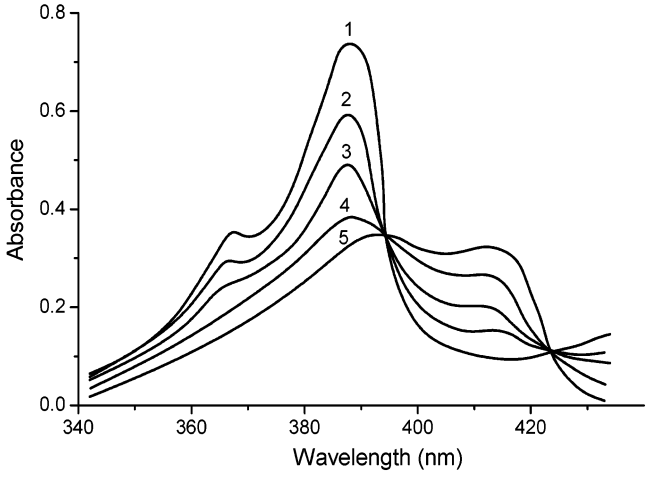

FIGURE 6. Conversion of CMA^+ (1.0×10^{-5} M) to MA at pH = 8.5 followed by the recording of absorption spectra at 45−65 (**1**), 90−110 (**2**), 135−155 (**3**) and 225−245 (**4**) time intervals (in s) following the mixing of the reagents; the absorption spectrum of MA (1.0×10^{-5} M) is given by (**5**).

yield MA* (**14**) (step XVIII*). Pathway four reflects the direct elimination of OCNH from **3** without a cyclic intermediate (step XV*). One can imagine that either OCNH or NCOH occur as products of steps XV(XV*) or XVIII (XVIII*). We assumed that OCNH is formed, since it is thermodynamically more stable than the other isomer by −22.3 kcal/mol (DFT level). To complete the picture, we also considered what would happen if OOH^- were first to attack the carbon atom of the cyano group in CMA^+ (steps II and III), with the intermediate products (**4** and **5**) then being converted to MA* (steps XVI, XVII and XVIII*). Now OH^- anions are not involved in pathways three and four, so if the activation barriers corresponding to steps XV or VII and XVIII were moderate, this could account for the long-lasting chemiluminescence observed in weakly acidic and neutral solutions.

The theoretically predicted thermodynamic data for all the reaction steps are given in Table 1, while Table 2

TABLE 2. Kinetic Characteristics of the Elementary Steps in the Reaction of CMA^+ with OOH^- and OH^- [a]

	gaseous phase						aqueous phase	
step no.	$\Delta_{a,298}H°$		$\Delta_{a,298}G°$		$_{298}k°$ ($_{298}\tau$ °$_{99}$)		$\Delta_{a,298}H°$	$\Delta_{a,298}G°$
(Schemes 1 and 2)	PM3	DFT	PM3	DFT	PM3	DFT	PM3 (COSMO)	DFT (PCM)
VII	83.2		84.4		8.1×10^{-50} (5.7×10^{49})		76.2	
IX	10.3		10.1		2.6×10^{5} (1.8×10^{-5})		15.7	
X	3.0		2.8		5.3×10^{10} (8.7×10^{-11})		17.2	
XII		3.5		3.9		8.3×10^{9} (5.5×10^{-10})		1.8
XIV	1.2	4.8	1.3	5.5	6.7×10^{11} (6.9×10^{-12})	5.4×10^{8} (8.6×10^{-9})	27.2	10.6
XV[b]	48.8	50.8	49.3	51.6	4.3×10^{-24} (1.0×10^{24})	9.8×10^{-26} (4.7×10^{25})	47.9	50.6
XVIII	33.8	28.5	33.3	28.4	2.5×10^{-12} (1.8×10^{12})	9.8×10^{-9} (4.7×10^{8})	35.5	27.1
XX	11.7	2.5	10.4	2.0	1.5×10^{5} (3.1×10^{-5})	2.0×10^{11} (2.3×10^{-11})	33.6	5.2
XXI	52.0	34.1	51.0	31.5	2.5×10^{-25} (1.8×10^{25})	5.2×10^{-11} (8.9×10^{10})	45.4	28.4
XXIII	22.0	13.0	22.0	12.7	4.9×10^{-4} (9.4×10^{3})	3.2×10^{3} (1.4×10^{-3})	24.1	18.2

[a] All characteristics apply to processes involving molecules in the ground electronic state. $\Delta_{a,298}H°$ and $\Delta_{a,298}G°$ (both in kcal/mol) represent the enthalpy and Gibbs' free energy (gaseous phase) or free energy (aqueous phase) of activation, respectively, at temperature 298.15 K and standard pressure (1 atm). $_{298}k°$ (in s^{-1}) and $_{298}\tau$ °$_{99}$ (in s) respectively denote the rate constant and the time after which the reaction is 99% complete. [b] Activation barriers correspond to the HOCN elimination from **3**.

contains kinetic data for the steps involving molecules in the ground electronic state. Additionally, the PM3- and DFT-optimized geometries originating from the acridine molecules produced by the reaction of CMA^+ with OOH^- or OH^- are shown in Figures S1 (lowest energy structures) and S2 (transition state structures) in the Supporting Information. We noted earlier,[8] and have confirmed in our present calculations, that the activation barriers to the addition of OOH^- or OH^- to CMA^+, **3** and **7**, as well as the hydrogen abstraction reactions are negligible. Such processes are thus not rate-determining steps, and we have not mentioned the activation barriers to them in Table 2. The thermodynamic and kinetic characteristics set out in Tables 1 and 2 allow one to conclude that pathways one and two mentioned above are the most probable routes by which CMA^+ is converted to MA* in alkaline media, while pathway four seems the most likely route by which the cation is oxidized by hydrogen peroxide in weakly acidic and neutral media. The OOH^- anions required for the process are available in small quantities under the latter conditions, since H_2O_2 exhibits the properties of a weak acid.[45] On considering these pathways, we were unable to find the structure of intermediate **13** by the DFT method; nevertheless, at this level we did locate the transition state structure for the direct conversion of **11** to 10-methyl-9-acridinone. Which of the pathways — one or two — is more probable is difficult to say: both are thermodynamically equally probable, although kinetics favors pathway one. The fact that the activation barrier to step VII is very high probably excludes pathway three as the one responsible for long-lasting chemiluminescence in weakly acidic or alkaline media. Nevertheless, as weak chemiluminescence in such conditions is observed, we think that this may have its origins in step XV, which has to overcome a lower activation barrier than does step VII. (We were able to locate the transition state only for the elimination of HOCN, and not the more stable OCNH, from **3**, which suggests that the actual barrier might be lower.) The overall values of the thermodynamic functions for pathways one, two and four are high enough to ensure electronic excitation of the 10-methyl-9-acridinone formed. As primary attack of OOH^- on the carbon atom of the cyano group in CMA^+ is not very probable, for the reasons mentioned above, we do not think that the pathway initiated by this process contributes to the overall processes by which MA* is formed.

Behavior of CMA^+ in Alkaline Media. OH^-, like OOH^-, can attack carbon atom (9) or carbon atom (15). The addition of OH^- to C(9), more probable for the reasons mentioned above, leads to **7** (step IV), which, via the elimination of HCN could be converted to MA (step XXI). Step IV is highly and step XXI slightly exothermic (Table 1), which would make this pathway probable if not for the relatively high activation barrier to the latter step (Table 2). In this situation we considered two other pathways of the nonradiative conversion of CMA^+ to MA in alkaline solutions: one involving steps IV, XIX, and XX and the other steps IV, XXII, and XXIII. The overall changes in the thermodynamic functions for both of these pathways are comparable and favor the conversion of **1** to **16**. Furthermore, the activation barrier to step XX is moderate (Table 2), which means that CMA^+ is most probably converted to MA via the initial abstraction of a proton by OH^- from the OH group of intermediate **7** and the subsequent elimination of CN^- (this pathway accounts for the results shown in Figure 6). This pathway is similar to pathway one, which describes the oxidation of CMA^+ with OOH^-, accompanied by chemiluminescence. Comparison of the activation barriers to step IX or XII and XX shows, however, that they are generally higher in the latter case, i.e., the nonradiative conversion of CMA^+ to MA in alkaline media (the reverse tendency is noted only in the case of values relevant to the PM3-

(COSMO) level). This explains the mechanism by which chemiluminescence is generated in the reaction of CMA^+ with OOH^- in alkaline media, as well as the relatively fast conversion of the cation to MA in the absence of hydrogen peroxide in the system.

For the above reasons, neither **8** nor **9** are likely precursors of MA. We did, however, consider pathways V, VI, and XXIV, to complete the picture of possible reactions of CMA^+ with OH^-.

The lowest energy and transition-state structures containing an acridine moiety occurring in all the steps indicated in Schemes 1 and 2 are depicted in the Supporting Information (Figures S1 and S2). However, intermediate and transition-state molecules could not be found for all of them at both levels of theory. The values in Tables 1 and 2, as well as the structures in Figures S1 and S2 (in the Supporting Information) correspond to the steps which we have been able to locate by carrying out geometry optimizations.

4. Concluding Remarks

CMA^+ reacts with hydrogen peroxide in weakly acidic, neutral and alkaline media producing MA*, which emits radiation. The processes leading to chemiluminescence in alkaline media are initiated by the attack of OOH^- on carbon atom (9) of CMA^+, followed by the abstraction of a proton by OH^- from the OOH group or, less probably, by the addition of OH^- to the carbon atom of the cyano group of **3** and the subsequent elimination of OCN^- and H_2O. Thus, short-lived chemiluminescence (in alkaline media) is generated via pathways involving steps I, VIII, and XII* or, to some extent, I, XIII, and XIV*. By contrast, long-lasting chemiluminescence (in weakly acidic and neutral media) is most probably generated via the pathway involving step XV*, i.e., via the direct elimination of OCNH from intermediate **3**.

In alkaline media and in the absence of hydrogen peroxide, CMA^+ is most probably converted to MA via the addition of OH^- to its carbon atom (9), followed by the abstraction of a proton by OH^- from the OH group of **7** and the subsequent elimination of CN^- (steps IV, XIX, and XX).

The conversion of CMA^+ to MA* in the presence of hydrogen peroxide creates a basis for its analytical use. CMA^+ is a very promising chemiluminogen since it reacts relatively easily with OOH^- in alkaline media. This is due to the moderate activation barriers to the rate determining steps. It can be seen from both experiment and calculations that CMA^+ is stable in acidic media and converts relatively easily to MA in strongly alkaline media. On the other hand, a moderately basic medium is required to initiate efficient chemiluminescence in the reaction of CMA^+ with OOH^-. It is thus important to select the appropriate conditions for the analytical procedures. Basic information on how this can be done is provided by Figures 3 and 4. They demonstrate that the total integral intensity of emission is mainly influenced by pH and the H_2O_2 concentration. As mentioned above, an increase in pH initially gives rise to greater quantities of OOH^-, which are necessary to initiate the processes leading to formation of MA*, but higher pH values facilitate conversion of CMA^+ to MA. On the other hand, both OH^- and OOH^- (or H_2O_2) can quench MA* and bring about its nonradiative deactivation. The emission intensities shown in Figures 3 and 4 are thus the result of both chemical processes (depicted in Scheme 1) and physical processes, which are not included in the mechanism we have suggested. More on the analytical utility of CMA^+ will be found in a recent publication of ours, which demonstrates its possible uses for determining N-, O-, and S-containing nucleophiles.[45]

The present work is an example of the successful use of theory to explain experimental facts. It has been shown that experimental findings are rationally described by the results of calculations, and the suggested mechanism forms a convenient basis on which to consider the chemiluminogenic features of the analytically useful reagent, the 9-cyano-10-methylacridinium cation. The investigations undertaken thus open up prospects for the widespread application of this compound.

Acknowledgment. The financial support of this work from the Polish State Committee for Scientific Research (KBN) through Grant No. 7 T09A 131 20 (Contract No. PB 1243/T09/2001/20) is gratefully acknowledged.

Supporting Information Available: Geometries of all stationary points and transition states in both Cartesian coordinates and diagrammatic form, the energies of stationary points, zero-point energies, and the number of imaginary frequencies for transition states. This material is available free of charge via the Internet at http://pubs.acs.org.

JO0354387